A Novel Craniotomy Simulation System for Evaluation of Stereo-pair Reconstruction Fidelity and Tracking

Xiaochen Yang[1,5], Logan W. Clements[2,5], Rebekah H. Conley[2,5], Reid C. Thompson[3,5], Benoit M. Dawant[1,4,5], and Michael I. Miga[2,3,4,5]

[1]Vanderbilt University, Department of Electrical Engineering and Computer Science, Nashville, TN USA
[2]Vanderbilt University, Department of Biomedical Engineering, Nashville, TN USA
[3]Vanderbilt University Medical Center, Department of Neurological Surgery, Nashville, TN USA
[4]Vanderbilt University Medical Center, Department of Radiology, Nashville, TN USA
[5]Vanderbilt Institute in Surgery and Engineering, Nashville, TN, USA

ABSTRACT

Brain shift compensation using computer modeling strategies is an important research area in the field of image-guided neurosurgery (IGNS). One important source of available sparse data during surgery to drive these frameworks is deformation tracking of the visible cortical surface. Possible methods to measure intra-operative cortical displacement include laser range scanners (LRS), which typically complicate the clinical workflow, and reconstruction of cortical surfaces from stereo pairs acquired with the operating microscopes. In this work, we propose and demonstrate a craniotomy simulation device that permits simulating realistic cortical displacements designed to measure and validate the proposed intra-operative cortical shift measurement systems. The device permits 3D deformations of a mock cortical surface which consists of a membrane made of a Dragon Skin® high performance silicone rubber on which vascular patterns are drawn. We then use this device to validate our stereo pair-based surface reconstruction system by comparing landmark positions and displacements measured with our systems to those positions and displacements as measured by a stylus tracked by a commercial optical system. Our results show a 1mm average difference in localization error and a 1.2mm average difference in displacement measurement. These results suggest that our stereo-pair technique is accurate enough for estimating intra-operative displacements in near real-time without affecting the surgical workflow.
Keywords: Craniotomy simulation, brain shift, intra-operative imaging, stereo-pair reconstruction, tracking, accuracy

1. INTRODUCTION

In traditional craniotomy, surgeons rely on pre-operative images, e.g., computed tomography (CT) and magnetic resonance imaging (MRI), to plan and execute the procedure. The development of computer modeling strategies permits addressing a major problem, which is the deformation of the brain that occurs as soon as the dura is opened and during surgery. In the recent past, a method that permits the updating of preoperative image volumes to compensate for brain shift using sparse data acquired intra-operatively and computer models has been proposed [1]. The methodology constructs a patient-specific finite-element model that can incorporate deformation-inducing events such as sag, swelling, hyperosmotic drug-induced shift, tissue retraction, and resection with high accuracy. The intra-operative data is used to update the preoperative image by measuring the tissue deformation, and applying corrections to neuro-navigation. The acquisition of intra-operative information that is required to drive these model-based compensation methods can vary in a number of ways, e.g. intra-operative MRI/CT, LRS, or stereo-pair images, all of which enhance the visualization of brain deformation during the surgery. However, there is always a tradeoff between obtaining more information, the impact to the workflow, and the effectiveness of the information. Intra-operative MR scanners are not common because

Medical Imaging 2016: Image-Guided Procedures, Robotic Interventions, and Modeling,
edited by Robert J. Webster, III, Ziv R. Yaniv, Proc. of SPIE Vol. 9786, 978612

they require operating rooms (OR) that are specially equipped. They also typically require moving the patient or equipment thus complicating the procedure and affecting the surgical workflow [2][3]. In addition, images in iMR are typically of considerably different resolution so one must still develop novel registration algorithms to register preoperative information to the intraoperative state. LRS takes advantages of its lightweight and compact size and is easily adaptable to the OR. At our institution we have employed a tracked LRS that is equipped with a high-resolution digital camera that can acquire a 3D cortical surface as well as a color image of the field of view [4][5][6][7]. However, performing one LRS surface sweep takes about 30 seconds during which the surgery needs to be interrupted. In addition, with each acquisition, the surgical microscope must be moved out of the field which does add further delay. Given the current frameworks with LRS, repeat and often scanning within the operating room is not practical at this time.. In work [4]-[7], the solution was to conduct data collection using LRS only at the beginning and ending stage of the surgery and estimating the displacement of features on cortical surface between the two states. Even though this operation affects little on the whole process of surgery, a substantial amount of intraoperative information is lost and in some cases data can be compromised by how much the cortical surface has changed. Another method that circumvents this is the use of stereo-pair images obtained from stereo-pair cameras embedded within surgical microscope platforms. These too can also potentially provide 3D cortical surface geometric point clouds in close to real time without disrupting the surgical workflow. In [8], [9], work has been done to evaluate the accuracy of stereo cameras but it was done on static phantoms. In this work, we evaluate the accuracy of stereo-pair-based surface reconstruction algorithms with a device we have designed to generate realistic cortical deformations compatible with those measured during tumor resection. The remainder of this paper describes both our device and its use for validating our stereo-pair method.

2. METHODS

Stereo-pair images or video streams that are necessary for camera calibration and 3D point cloud reconstruction are acquired using software we have developed in-house for this purpose [9]. Our novel craniotomy simulation device shown in Figure 1 is designed to permit in-plane stretching as well as out-of-plane deformation of a membrane to generate simulated brain shift. Ground truth displacements are measured with an optically tracked probe also shown in Figure 1. The membrane deformation computed using our camera-based systems is compared to displacements measured with the probe to assess its accuracy.

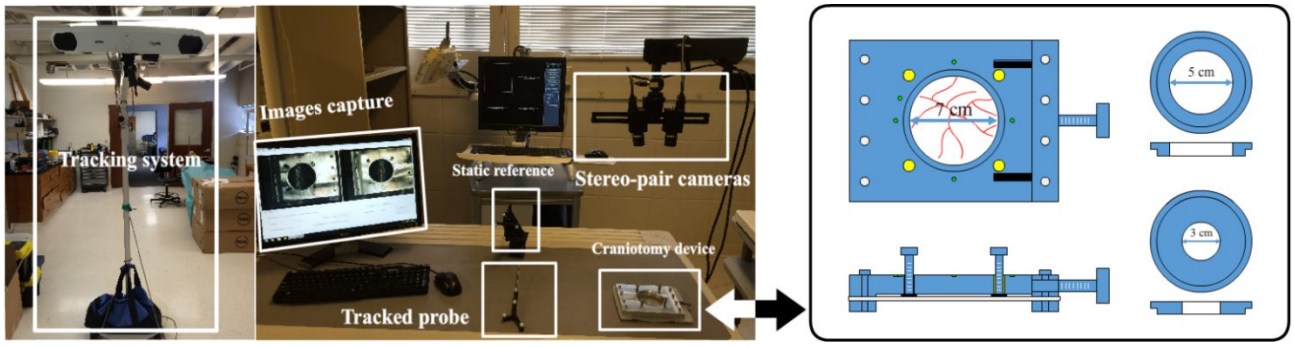

Figure 1. System overview and craniotomy device design

2.1. Apparatus

As shown in Figure 1, our experimental setup consists of a pair of cameras, a monitor that shows the captured images, an optical tracking system with a static reference and a stylus, and our novel craniotomy simulation device. We use two Grasshopper® IEEE-1394b (FireWire) digital cameras (GRAS-20S4C-C), which are equipped with a Sony ICX274 CCD with a resolution of 1624 x 1224. These cameras provided by Point Grey Research, Inc. (Richmond, British

Columbia, Canada) can acquire videos at 30 frames per second (FPS). The optical tracking system is a Polaris Spectra manufactured by Northern Digital, Inc. (Waterloo, Ontario, Canada). It is used to measure the ground-truth displacement manually with a tracked probe. The tracking accuracy for a Polaris Spectra is reported to be 0.25-0.3 mm RMS for an individual marker tracked within its working volume. With respect to stylus point localization, the accuracy of these tools is typically configuration dependent and is estimated to be approximately 0.5 mm in our case [10]. Our novel device is designed to simulate realistic displacements occurring during surgery. As Figure 1 shows, it has two circular rings inserts that can be placed in the device aperture to simulate different craniotomy sizes (at our institution the size of the craniotomy can vary substantially from surgeon to surgeon). The five hemispherical divots visible outside the main circle serve as fiducial points to register the mock cortical surface phantom device. The four screws on each side of the device act to clamp the silicon membrane. Using a lead-screw mechanism, the device clamp on the right side can be extended such that a systematic and even stretch of the silicon membrane can be imparted. This provides two cortical deformation behaviors typically seen in operating rooms, namely, change in lateral interpoint distances, and translation of some cortical surface laterally such that new structures become visible and some initially visible structures become obstructed with a translation under the bone. In addition to lateral motion, four additional medium-size screws are placed around the mock craniotomy and can push the membrane down more than 1cm to produce deformation patterns that are more complex than just stretching. More specifically, brain sag often manifests as a withdrawal of the brain surface into the cranium on average of 1cm (although it depends on patient head orientation). The membrane is marked with a realistic mock cortical vessel pattern and is made of Dragon Skin® high performance silicone rubber.

2.2. Camera Calibration

In this work we rely on a classical and widely-used method [11] for camera calibration. This technique requires acquisition of a series of images from a calibration pattern. We have used a planar checkerboard pattern that has 8 x 6 internal corners with each square of size 13.5 mm as shown in Figure 2. About eighteen pairs of images acquired from the calibration pattern in various positions and orientations are required to calibrate the images. To facilitate acquisition, we have developed a user-friendly graphical user interface (GUI) [12]. It is designed to work on all USB, Point Grey Research or other IEEE-1394b (FireWire) digital cameras.

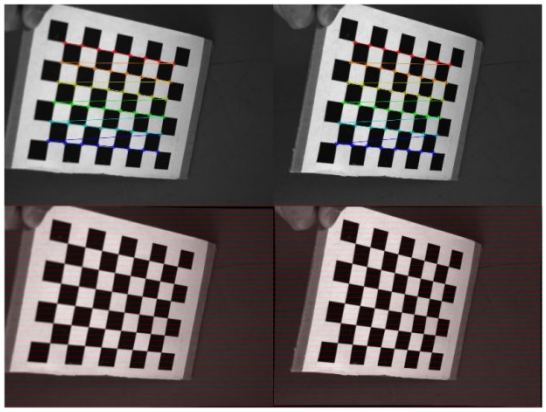

Figure 2. Checkerboard with detected corners and stereo rectification pair with epipolar line drawn in red

In order to compute intrinsic and extrinsic parameters of stereo-pair cameras, the epipolar geometry based on pinhole models is built to search for corresponding points in stereo matching. In Figure 3, Image plane $\boldsymbol{\pi_1}$and $\boldsymbol{\pi_2}$ are captured by two cameras whose center locates at point $\boldsymbol{C_1}$and $\boldsymbol{C_2}$ respectively. The image point $\boldsymbol{x_1}$and $\boldsymbol{x_2}$ represents the space point $\boldsymbol{X}$ in their image coordinates, which together are coplanar on epipolar plane $\boldsymbol{\pi}$ as well as camera centers $\boldsymbol{C_1}$and $\boldsymbol{C_2}$. The intersection of epipolar plane $\boldsymbol{\pi}$ with image plane $\boldsymbol{\pi_1}$and $\boldsymbol{\pi_2}$ is epipolar line $\boldsymbol{l_1}$and $\boldsymbol{l_2}$, while epipole $\boldsymbol{e_1}$and $\boldsymbol{e_2}$ is the intersection point of joining the camera centers with the image planes. The fundamental matrix F [13] is defined by

mapping a point in left image to its corresponding epipolar line of right image, which can also write algebraic representation as:

$$\boldsymbol{l_2} = F\boldsymbol{x_1} \tag{1}$$

The point $\boldsymbol{x_2}$ lying on line $\boldsymbol{l_2}$ satisfies:

$$\boldsymbol{x_2}^T\boldsymbol{l_2} = 0 \tag{2}$$

Substitute equation (1) in equation (2), then

$$\boldsymbol{x_2}^T F\boldsymbol{x_1} = 0 \tag{3}$$

Equation (3) demonstrates that F can also match a point from left image to the right one. The calibration image pairs provide a number of correspondences which is used to solve F by a least squares method [11]. The accuracy of calibration procedure can be checked by computing the distance between the corresponding corners and the estimated epipolar lines because we know the corresponding corner lies on the epipolar line in theory.

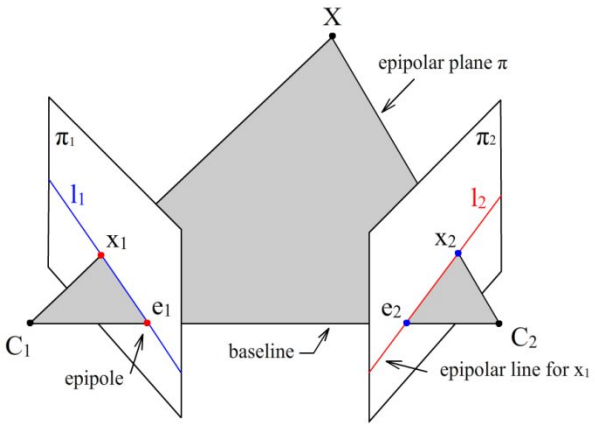

Figure 3. Epipolar geometry

2.3. Three-dimensional Reconstruction

The reconstruction procedure reprojects 2D image points to physical world positions. As shown in Figure 4, we have a parallel-aligned stereo pair $\boldsymbol{\pi_1}$and $\boldsymbol{\pi_2}$ that are coplanar and collinear with each other. The principal rays from camera centers $\boldsymbol{C_1}$and $\boldsymbol{C_2}$ perpendicular to the image planes intersect the planes on the principal points $\boldsymbol{p_1}$ and $\boldsymbol{p_2}$, which have been rectified to the same pixel coordinates in their respective left and right images. Image point $\boldsymbol{x_1}$ (x_1, y_1) and its corresponding point $\boldsymbol{x_2}$ (x_2, y_2) are collinear. The coordinates of point $\boldsymbol{x_2}$ in right image is exactly the same as point $\boldsymbol{x_2}'$ in the left image, so the disparity d is defined as:

$$d = x_1 - x_2 \tag{4}$$

The depth Z of world point $\boldsymbol{X}$ can be computed by similar triangles using:

$$\frac{T-d}{T} = \frac{Z-f}{f} \quad \Rightarrow \quad Z = \frac{fT}{d} \tag{5}$$

In (5), T is the horizontal distance between two camera centers $\boldsymbol{C_1}$and $\boldsymbol{C_2}$, and f is the focal length. For computation efficiency, the reprojection matrix Q is defined as below:

$$Q = \begin{bmatrix} 1 & 0 & 0 & -c_{x1} \\ 0 & 1 & 0 & -c_{y1} \\ 0 & 0 & 0 & f \\ 0 & 0 & -\frac{1}{T} & \frac{c_{x1} - c_{x2}}{T} \end{bmatrix} \tag{6}$$

Here, point $(c_{x1},\ c_{y1})$ is the principal point in left image, while c_{x2} is the x coordinate of the principal point in the right image. In frontal parallel configuration of stereo pair, the two principal rays intersect at infinity, and then $c_{x1} = c_{x2}$, which makes the bottom right corner term in (6) equal zero. The reprojection matrix Q reprojects a 2D homogeneous point (associated with disparity d) into a 3D point $(\frac{X}{W},\ \frac{Y}{W},\ \frac{Z}{W})$ in physical world by the following mapping:

$$Q \begin{bmatrix} x \\ y \\ d \\ 1 \end{bmatrix} = \begin{bmatrix} X \\ Y \\ Z \\ W \end{bmatrix} \tag{7}$$

In practice, the camera pair is seldom placed perfectly parallel-aligned, we need to mathematically rectify the left and right images into a coplanar and collinear configuration as well as synchronize two cameras in order to capture the image pair at the exact same time. There are mainly two different methods for rectification: one is Hartley's algorithm [14], which tries to find homographies that map the epipoles to infinity using just the fundamental matrix F. However, this method lacks sense of image scale because reconstruction result only depends on a projective transform, which means 3D objects with different scales may have the same 2D coordinates. The second one is Bouguet's algorithm [15][16], which is a completed and simplified version based on [11][17] that takes advantage of two calibrated cameras' rotation and translation parameters to minimize reprojection distortions as well as maximizing the view overlap area. Here, we choose Bouguet's algorithm in our implementation.

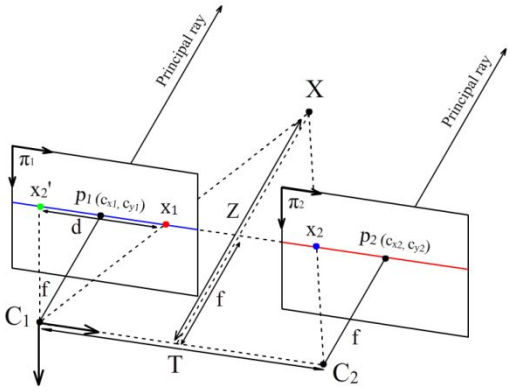

Figure 4. Reprojected triangulation of rectified stereo pair, and depth Z can be calculated by similar triangles

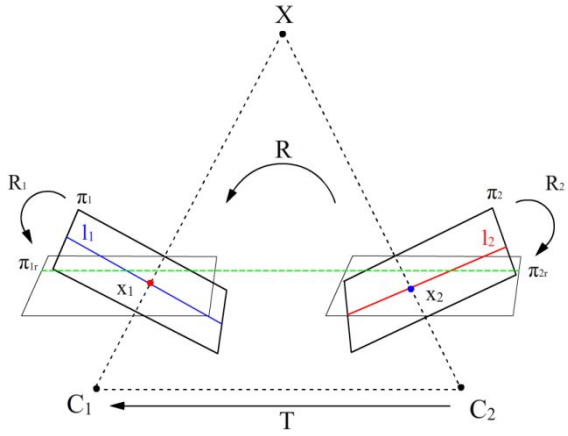

Figure 5. Mathematically adjust the stereo pair to a perfectly undistorted, row-aligned, frontal parallel configuration

In Figure 5, R is the rotation matrix from right image coordinates to the left one, then rectified rotation matrix R_1, R_2 and rectified camera matrix M_1, M_2 are computed by rotating the two principal rays parallel to each other and aligning the epipolar lines horizontally (as the green line shows). Known these matrices, the rectification map is constructed to rectify the image pair. After rectification is done, the disparity map is computed by finding the differences of x coordinates of the same features in rectified left and right images by applying block matching (BM) or semi-global block

matching (SGBM) or other methods [18]. 3D point clouds are then reconstructed directly from the disparity map based on equation (6) and (7) using the Open Computer Vision Library (OpenCV) SDK [19].

2.4. Experiment Prototype

The accuracy of our camera-based surface reconstructing and tracking system was tested with our craniotomy simulation device as follows (also see Figure 6):

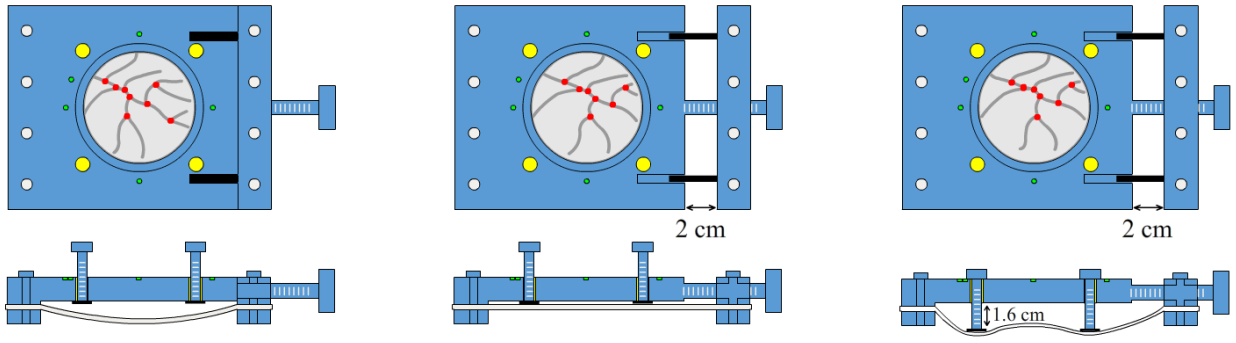

(a) Baseline (b) Stretch (c) Stretch + Sag

Figure 6. Experiment prototype of three states: baseline, stretch and stretch as well as sag

1. Calibrate the stereo-pair cameras using the checkerboard calibration pattern.
2. Place the mock cortical surface deformation device with clamped mock cortical surface under the camera pair, acquire images, and subsequently create a 3D point cloud.
3. Record the real world position of the five fiducial points around the mock craniotomy, as well as of 8 visible vessel target features on the membrane using the independent optically tracked stylus (one feature may disappear after stretching the device).
4. Take the device out of the field of view, and apply a stretch using the screw mechanism (Figure 6 (b)), then repeat steps 2 and 3.
5. Take the device out of the field of view, and apply the brain-sag simulated retreat of the mock brain surface using the four screws around the craniotomy (Figure 6 (c)), and then repeat step 2 and 3.
6. Once completed, the data above reflect three sets of optically digitized points (divots and vessels) using the stylus, as well as three point clouds. Using the divots, all data are registered to a common space (here, all datasets are registered to the baseline dataset acquired with the optical tracker). Position and displacement of vessel bifurcations measured by stylus and stereo pairs are then compared.

3. RESULTS

By computing the absolute distance between detected checkerboard corners and their epipolar lines on the other image we estimate our calibration error to be 0.3 pixels. A 3D point cloud of the device reconstructed from a stereo pair as well as the disparity map is shown in Figure 7. Table 1 reports differences in position and displacement for each landmark and each membrane state. Both the stereovision and tracking displacement is computed based on baseline state. Note that the row of target 1 is missing because stretching the membrane makes the feature near the border go out of view, which is reasonable since it may happen in real craniotomy. Mean target registration errors are approximately 1mm and mean displacement errors slightly above 1mm. These errors include the localization error associated with the optical tracking system and the error associated with registering the real world and the image spaces. By comparing known distances between landmarks on the physical phantom and distances measured with the tracking system, we estimate the

localization error of the optical stylus to be approximately 0.5mm, which is consistent with theoretical results [10]. A more rigorous study that will permit to estimate the localization error at the target points for our landmark and stylus configuration is ongoing. The displacement of the landmarks measured with the tracking system is shown on the 2D images in Figure 8 (top panels) and the corresponding 3D clouds are shown in the bottom panels. Red points indicate the position of eight features in baseline state, while green and yellow ones show their new places in stretch and stretch plus sag state respectively. We notice that there are only seven green and yellow points because of the stretching operation. The white arrows present the direction and magnification of the displacement from the baseline to each new state.

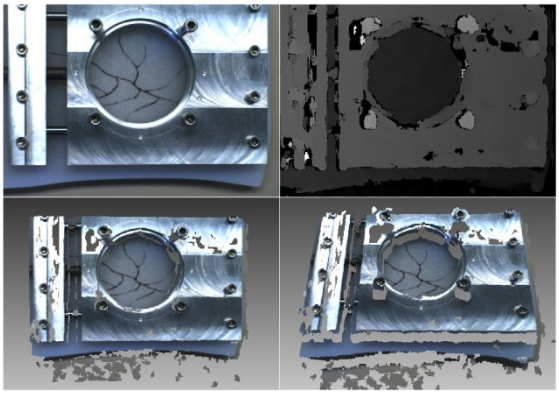

Figure 7. Craniotomy device with disparity image and point cloud reconstruction

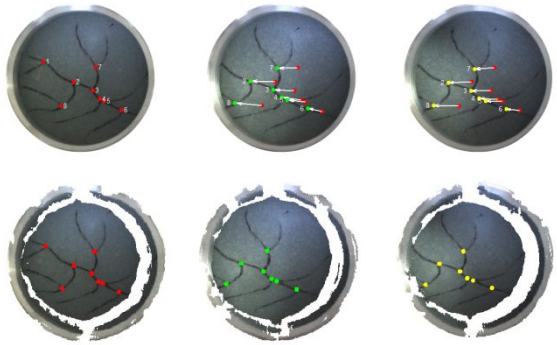

Figure 8. Displacement trajectories in 2D image (top) and corresponding 3D clouds (bottom)

Table 1. Displacement, error of displacement and error of localization between stereovision and tracking

Target Feature	Category	Stereovision Displacement	Tracking Displacement	Displacement Error	Target Registration Error
Target 2	Baseline	-	-	-	0.97
	Stretch	[-11.93 -0.29 -5.86]	[-11.78 -1.22 -5.31]	1.09	0.40
	Stretch + Sag	[-11.85 -0.58 -0.99]	[-11.43 -1.09 -0.68]	0.73	0.61
Target 3	Baseline	-	-	-	0.82
	Stretch	[-9.96 0.16 -6.21]	[-9.62 -1.44 -6.31]	1.64	0.96
	Stretch + Sag	[-9.98 -0.24 -1.13]	[-9.75 -1.18 -1.82]	1.19	0.84
Target 4	Baseline	-	-	-	1.29
	Stretch	[-9.11 0.90 -6.00]	[-8.11 -1.19 -6.23]	2.33	1.25
	Stretch + Sag	[-9.55 0.33 -0.50]	[-8.97 -1.19 -1.27]	1.80	0.84
Target 5	Baseline	-	-	-	1.30
	Stretch	[-8.58 0.74 -5.80]	[-8.98 -0.30 -5.47]	1.16	1.41
	Stretch + Sag	[-8.54 0.08 -0.05]	[-8.87 -0.18 -0.38]	0.53	1.21
Target 6	Baseline	-	-	-	1.21
	Stretch	[-6.72 1.41 -5.33]	[-6.30 -0.39 -5.64]	1.87	1.86
	Stretch + Sag	[-6.77 0.65 0.86]	[-6.42 0.03 1.25]	0.81	1.01
Target 7	Baseline	-	-	-	0.72
	Stretch	[-9.83 -0.69 -6.30]	[-9.38 -0.67 -5.64]	0.79	0.87
	Stretch + Sag	[-9.75 -1.06 -1.27]	[-9.37 -0.74 -1.23]	0.49	0.96
Target 8	Baseline	-	-	-	1.83
	Stretch	[-13.22 0.89 -5.03]	[-14.35 1.00 -4.34]	1.32	0.60
	Stretch + Sag	[-13.13 0.17 0.48]	[-14.34 0.43 1.68]	1.72	0.12
Mean Error	-	-	-	1.24	0.99

4. CONCLUSIONS

We have built a novel craniotomy and cortical deformation simulation system that generates realistic soft tissue displacements. The device allows for measurements and comparisons between stereo-pair reconstructions and commercial tracking systems. The device can simulate known behaviors within the operating room theatre (namely lateral shift and sag). The different inserts designed allow for variable craniotomy size analysis that range from 3 to 7 cm. The comparison results indicate that the use of stereo-pair images captured from stereo cameras has the potential to gather valid intra-operative information without disrupting the surgery. This is the prerequisite for us to compensate brain shift using stereo-pair reconstruction fully-automatically in OR. We should note that while several groups are pursuing microscope driven stereo-pair cortical shift estimation, there is still a paucity of validation with respect to independent tracking method comparisons under controlled conditions. To our knowledge, the construction of a device like this is completely novel. To sum up, the purpose of this work was to evaluate the stereo-pair reconstruction fidelity as well as the manually-designated brain shift tracking with stereo pair. Results we have obtained suggest that the deformation computed from 3D cortical vessel surface similar to the deformation measured with the ground truth tracking system. Our future work is to use stereovision as a substitute for LRS in our preoperative and intraoperative computational pipeline for brain shift correction [20].

5. ACKNOWLEDGEMENTS

This work is funded by the National Institutes of Health, National Institute for Neurological Disorders and Stroke grant number R01-NS049251. We would also like to acknowledge Point Grey Research, Inc. and Northern Digital, Inc. for providing essential equipment and resources, and John Fellenstein from the Vanderbilt Machine Shop for his assistance in our cortical surface deformation simulation device.

REFERENCES

[1] M. I. Miga, D.W. Roberts, F.E. Kennedy, L.A. Platenik, A. Hartov, K.E. Lunn, and K.D. Paulsen, "Modeling of retraction and resection for intraoperative updating of images," Neurosurgery, vol. 49, no. 1, pp. 75-85, Oct. 2001.

[2] Clatz, H. Delingette, I. Talos, A. J. Golby, R. Kikinis, F. A. Jolesz, N. Ayache, and S. K. Warfield, "Robust non-rigid registration to capture brain shift from intra-operative MRI," IEEE Trans. Med. Imag., vol. 24, no. 11, pp.1417–1427, Nov. 2005.

[3] N. Archip, O. Clatz, S. Whalen, D. Kacher, A. Fedorov, A. Kot, N. Chrisochoides, F. Jolesz, A. Golby, P. M. Black, and S. K. Warfield, "Non-rigid alignment of pre-operative MRI, fMRI, and DT-MRI with intra-operative MRI for enhanced visualization and navigation in imageguided neurosurgery," NeuroImage, vol. 35, pp. 609–624, Apr. 2007.

[4] M. I. Miga, T.K. Sinha, D.M. Cash, R.L. Galloway, and R.J. Weil, "Cortical surface registration for image-guided neurosurgery using laserrange scanning," IEEE Trans. Med. Imag., vol. 22, no. 8, pp. 973–985, Aug. 2003.

[5] S. Ding, M. I. Miga, R. C. Thompson, P. Dumpuri, A. Cao, and B. M. Dawant, "Estimation of intra-operative brain shift using a laser range scanner," in Proc. IEEE Eng. Med. Biol. Soc., 2007, pp. 848–851.

[6] A. Cao, R.C. Thompson, P. Dumpuri, B.M. Dawant, R.L. Galloway,S. Ding, and M.I. Miga, "Laser range scanning for image-guided neurosurgery:Investigation of image-to-physical space registrations," Med.Phys., vol. 35, pp. 1593–1605, Apr. 2008.

[7] T. K. Sinha, V.Duay, B.M. Dawant, and M.I. Miga, "Cortical shift tracking using laser range scanner and deformable registration methods," in Lecture Notes in Computer Science: Springer-Verlag, 2003, Medical Image Computing and Computer Assisted Intervention, vol. 2879. New York, Springer-Verlag, 2009, pp. 166–174.

[8] A. N. Kumar, T.S. Pheiffer, A.L. Simpson, R.C. Thompson, M.I. Miga, and B.M. Dawant, “Phantom-based comparison of the accuracy of point clouds extracted from stereo cameras and laser range scanner,” In Proc. of SPIE Medical Imaging: Image-guided Procedures, Robotic Interventions, and Modeling, 2013, 867125.

[9] A. N. Kumar, M.I. Miga, T.S. Pheiffer, L.B. Chambless, R.C. Thompson, and B.M. Dawant, “Persistent and automatic intraoperative 3D digitization of surfaces under dynamic magnifications of an operating microscope,” Medical Image Analysis, Vol. 19, No. 1, pp. 30-45, January 2015.

[10] J. B. West, C.R. Maurer, “Designing optically tracked instruments for image-guided surgery”. IEEE Trans Med Imag. 2004;23, no. 5:533–545

[11] Z. Zhang, “A flexible new technique for camera calibration,” IEEE Transactions on Pattern Analysis and Machine Intelligence, vol. 22, no. 11, pp. 1330-34, Nov. 2000.

[12] X. Yang, “Stereo-pair Capture Software”, Vanderbilt.edu, https://my.vanderbilt.edu/xiaochen/archives/75 (accessed 10 August 2015).

[13] R. Hartley and A. Zisserman. 2003. Multiple View Geometry in Computer Vision (2 ed.). Cambridge University Press, New York, NY, USA.

[14] R. I. Hartley, “Theory and practice of projective rectification,” InternationalJournal of Computer Vision 35 (1998): 115–127.

[15] J. Y. Bouguet, "Visual methods for three-dimensional modeling," Ph.D. Thesis, California Institute of Technology.

[16] J. Y. Bouguet, “Camera calibration toolbox for Matlab”, http://www.vision.caltech.edu/bouguetj/calib_doc/ (accessed 10 August 2015).

[17] R. Y. Tsai, “A versatile camera calibration technique for high accuracy 3D machinevision metrology using off-the-shelf TV cameras and lenses,” IEEE Journal ofRobotics and Automation 3 (1987): 323–344.

[18] D. Scharstein, and R. Szeliski. 2002. A taxonomy and evaluation of dense two-frame stereo correspondence algorithms. International Journal of Computer Vision 47, 7-42.

[19] G. Bradski, and A. Kaehler, "Learning OpenCV: Computer Vision with the OpenCV Library," O'Reilly Media, pp. 370-458, 2008.

[20] K. Sun, T.S. Pheiffer, A.L. Simpson, J.A. Weis, R.C. Thompson, M.I. Miga, "Near Real-Time Computer Assisted Surgery for Brain Shift Correction Using Biomechanical Models," Translational Engineering in Health and Medicine, IEEE Journal of , vol.2, no., pp.1,13, 2014 vol. 8671, pp. 867125.